Loss-of-function variants in *TIAM1* are associated with developmental delay, intellectual disability, and seizures

Graphical abstract

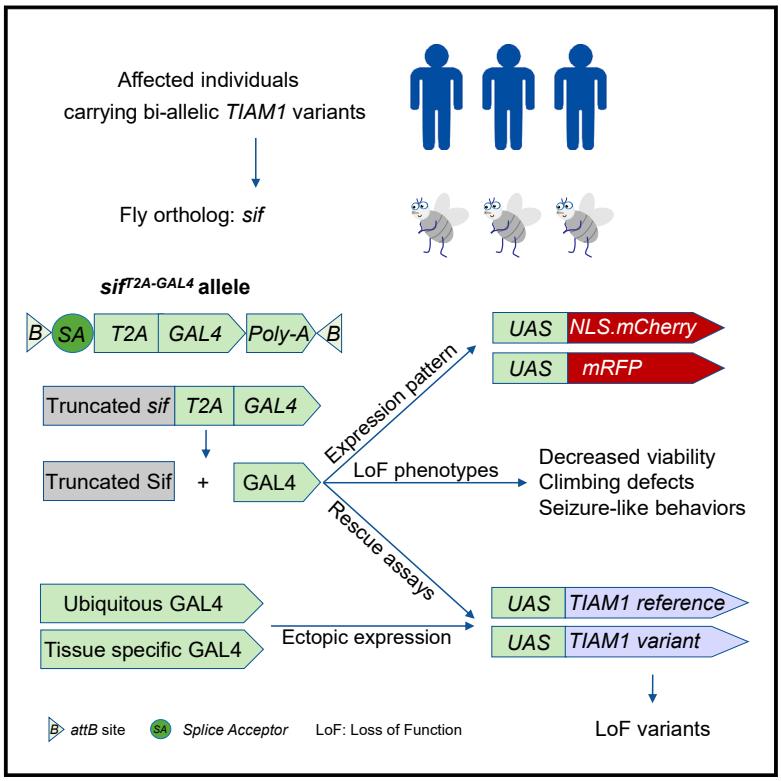

Authors

Shenzhao Lu, Rebecca Hernan, Paul C. Marcogliese, ..., Maria J. Guillen Sacoto, Wendy K. Chung, Hugo J. Bellen

Correspondence

wkc15@cumc.columbia.edu (W.K.C.), hbellen@bcm.edu (H.J.B.)

Lu et al., 2022, The American Journal of Human Genetics *109*, 571–586
April 7, 2022
https://doi.org/10.1016/j.ajhg.2022.01.020

Loss-of-function variants in *TIAM1* are associated with developmental delay, intellectual disability, and seizures

Shenzhao Lu,[1,2,3] Rebecca Hernan,[4] Paul C. Marcogliese,[1,2] Yan Huang,[1,2] Tracy S. Gertler,[5] Meltem Akcaboy,[6] Shiyong Liu,[7] Hyung-lok Chung,[1,2] Xueyang Pan,[1,2] Xiaoqin Sun,[7] Melahat Melek Oguz,[6] Ulkühan Oztoprak,[8] Jeroen H.F. de Baaij,[9] Jelena Ivanisevic,[5] Erin McGinnis,[5] Maria J. Guillen Sacoto,[10] Wendy K. Chung,[4,11,*] and Hugo J. Bellen[1,2,*]

Summary

TIAM Rac1-associated GEF 1 (TIAM1) regulates RAC1 signaling pathways that affect the control of neuronal morphogenesis and neurite outgrowth by modulating the actin cytoskeletal network. To date, *TIAM1* has not been associated with a Mendelian disorder. Here, we describe five individuals with bi-allelic *TIAM1* missense variants who have developmental delay, intellectual disability, speech delay, and seizures. Bioinformatic analyses demonstrate that these variants are rare and likely pathogenic. We found that the *Drosophila* ortholog of *TIAM1*, *still life* (*sif*), is expressed in larval and adult central nervous system (CNS) and is mainly expressed in a subset of neurons, but not in glia. Loss of *sif* reduces the survival rate, and the surviving adults exhibit climbing defects, are prone to severe seizures, and have a short lifespan. The *TIAM1* reference (Ref) cDNA partially rescues the *sif* loss-of-function (LoF) phenotypes. We also assessed the function associated with three *TIAM1* variants carried by two of the probands and compared them to the *TIAM1* Ref cDNA function *in vivo*. *TIAM1* p.Arg23Cys has reduced rescue ability when compared to *TIAM1* Ref, suggesting that it is a partial LoF variant. In ectopic expression studies, both wild-type *sif* and *TIAM1* Ref are toxic, whereas the three variants (p.Leu862Phe, p.Arg23Cys, and p.Gly328Val) show reduced toxicity, suggesting that they are partial LoF variants. In summary, we provide evidence that *sif* is important for appropriate neural function and that *TIAM1* variants observed in the probands are disruptive, thus implicating loss of *TIAM1* in neurological phenotypes in humans.

Introduction

Many patients with rare diseases undergo a long and frustrating journey to obtain an accurate diagnosis, often referred to as the diagnostic odyssey. Whole-exome sequencing (WES) and whole-genome sequencing (WGS) are effective approaches to identify diagnoses, as 80% or more of rare diseases are estimated to be caused by genomic abnormalities.[1,2] However, these comprehensive sequencing methods also uncover many variants of uncertain significance (VUSs) with unknown clinical impact.[3] *Drosophila melanogaster* allows effective approaches to probe the functional impacts of these variants.[4]

Here, we argue that bi-allelic loss-of-function (LoF) variants of TIAM Rac1-associated GEF 1 (*TIAM1* [MIM: 600687]) cause a disease associated with developmental delay, intellectual disability, speech delay, and seizures. TIAM1 is a guanine nucleotide exchange factor (GEF).[5–9] GEFs are positive regulators of small GTPases that promote their activation. Each individual GEF has a specificity profile,[8] and TIAM1 is a Ras-related C3 botulinum toxin substrate 1 (RAC1)-specific GEF.[6] RAC1 stimulates signaling pathways that regulate actin cytoskeleton organization, cell movement, differentiation, and proliferation.[5]

TIAM1 is enriched in the brain.[10,11] The rodent ortholog, *Tiam1*, is also expressed in the brain, is present in dendrites and spines, and is required to maintain proper outgrowth during development.[7] When activated by neurotrophins such as brain-derived neurotrophic factor (BDNF), the TRKB receptor binds and activates TIAM1, which in turn activates RAC1, causing morphological changes by increasing neurite outgrowth.[12,13] Similarly, when glutamate activates N-methyl-D-aspartate (NMDA) receptors, TIAM1 is also activated to control actin remodeling by inducing RAC1-dependent pathways.[7,12] The localization of TIAM1 to spines is regulated by par-3 family cell polarity regulator and thereby controls proper spine formation.[14] Mice lacking *Tiam1* have simplified dendritic arbors, reduced dendritic spine density, and diminished excitatory synaptic transmission in the dentate gyrus.[15] Taken together, TIAM1 controls neuronal morphogenesis and neurite outgrowth by RAC1-dependent

[1]Department of Molecular and Human Genetics, Baylor College of Medicine, Houston, TX 77030, USA; [2]Jan and Dan Duncan Neurological Research Institute, Texas Children's Hospital, Houston, TX 77030, USA; [3]Howard Hughes Medical Institute, Baylor College of Medicine, Houston, TX 77030, USA; [4]Department of Pediatrics, Columbia University, New York, NY 10032, USA; [5]Division of Neurology, Department of Pediatrics, Ann & Robert H. Lurie Children's Hospital of Chicago, Chicago, IL 60611, USA; [6]Department of Pediatrics, Dr. Sami Ulus Maternity and Children's Health and Diseases Training and Research Hospital, Ankara, Turkey; [7]Department of Neurosurgery, Xinqiao Hospital, Army Medical University, Chongqing, 400037, PR China; [8]Department of Pediatric Neurology, Dr. Sami Ulus Maternity and Children's Health and Diseases Training and Research Hospital, Ankara, Turkey; [9]Department of Physiology, Radboud University Medical Center, Radboud Institute for Molecular Life Sciences, Nijmegen, 6500HB, the Netherlands; [10]GeneDx, Inc., Gaithersburg, MD 20877, USA; [11]Department of Medicine, Columbia University Medical Center, New York, NY 10032, USA
*Correspondence: wkc15@cumc.columbia.edu (W.K.C.), hbellen@bcm.edu (H.J.B.)
https://doi.org/10.1016/j.ajhg.2022.01.020.

actin cytoskeletal remodeling in rodents. However, alterations in *TIAM1* have not yet been reported in the Online Mendelian Inheritance in Man (OMIM) database or the literature as causing human disease.[16]

still life (*sif*) encodes the ortholog of *TIAM1* in *Drosophila*.[10,17] Previous studies showed that loss of *sif* leads to reduced locomotor activity.[18,19] Sif was reported to be localized presynaptically and shown to genetically interact with Fasciclin II, a neural cell-adhesion molecule localized pre- and postsynaptially that controls synaptic growth, stabilization, and presynaptic structural plasticity.[19–21] Its partial loss causes loss of some boutons at neuromuscular junctions.[19] Also, Sif is highly enriched in lens-secreting cells in fly eyes and affects the distribution pattern of E-cadherin in pupal eyes.[22]

Here, we identified bi-allelic *TIAM1* missense variants in five individuals from four families with developmental delay, intellectual disability, speech delay, and seizures. Functional studies in *Drosophila* revealed that the loss of *sif* reduces the survival rate of flies, and the surviving adult flies have a remarkably reduced lifespan and exhibit severe climbing defects. In addition, *sif* LoF mutants display severe seizure-like behaviors when stressed. Expression of the human *TIAM1* reference (*TIAM1* Ref) cDNA partially rescues the lethality of *sif* LoF mutants, whereas the variants observed in probands behave as partial LoF mutations in different phenotypic assays. Our data support the hypothesis that the variants observed in the probands are the cause of the observed phenotypes.

Material and methods

Human genetics

This study was approved by the institutional review board at Columbia University. Legal guardians of affected individuals provided informed consent. Five individuals, including a pair of monozygotic (MZ) twins, with developmental delay/intellectual disabilities from four independent families had trio clinical exome sequencing.

Exome sequencing

Using genomic DNA from the proband and parents, the exonic regions and flanking splice junctions of the genome were captured using the IDT xGen Exome Research Panel v1.0 (Integrated DNA Technologies, Coralville, IA). Massively parallel (next-generation) sequencing was done on an Illumina sequencer with 100 bp or greater paired-end reads. Reads were aligned to human genome build GRCh37/UCSC hg19 and analyzed for sequence variants using a custom-developed analysis tool. Additional sequencing technology and variant interpretation protocol have been previously described.[23] The general assertion criteria for variant classification are publicly available on the GeneDx ClinVar submission page (see web resources). Trio WES of proband 4 and parents was done and analyzed at Chigene, Beijing, China.

Drosophila stocks and maintenance

All fly strains used in this study were generated in house or obtained from the Bloomington *Drosophila* Stock Center (BDSC). The $sif^{T2A\text{-}GAL4}$ allele was created by conversion of a MiMIC (Minos-mediated integration cassette)[24] insertion line, *y[1] w[*]; Mi{y[+mDint2] = MIC}sif[MI02376]* (BDSC, 35834) via recombination-mediated cassette exchange (RMCE) as described.[25,26] $sif^{T2A\text{-}GAL4}$ LoF mutants were rescued with fly *sif* cDNA *P{w[+mC] = UAS-sif.S} 2.1* (BDSC, 9128). For complementation tests, immunostaining, and RNAi assays, see genotypes in Table S1. *elav-GAL4*, *UAS-Empty*, and *UAS-lacZ* were published previously.[27,28]

Drosophila behavioral assays

For the climbing assay,[29] flies were transferred to an empty vial, the flies were tapped to the bottom of the vial, and their climbing ability (negative geotaxis) was measured. Climbing distance was measured (15 cm as maximum). Flies were allowed to climb for 20 s. If some of the fly groups did not show obvious climbing defects, another unbiased method was used by assessing the time for flies to climb vertically to 4 cm.[30]

For the bang-sensitivity assay,[31] flies were transferred to an empty vial and vortexed at maximum speed for 10 s, and the time to recovery to freely moving status (without abnormal falling or flipping) was measured. For the heat shock assay,[32] flies were transferred to an empty vial and submerged in a 42°C water bath for 30 s. We measured the percentage of flies that were unable to keep an upright position. We then measured the time to recovery to a freely moving status. In these assays, we record for only 30 s. Flies that do not recover within 30 s are recorded at the 30 s time point even if they require many more seconds or minutes to recover.

For survival rate, the surviving adult flies within 1 day of eclosion were counted, and each genotype was identified to assess Mendelian ratios. For lifespan, freshly eclosed flies were separated and maintained at 18°C, and survival was determined every other day.

Generation of human UAS-TIAM1 transgenic lines

Human *UAS-TIAM1* lines were generated as described.[33,34] The *TIAM1* cDNA clone corresponds to GenBank: NM_001353694, which encodes the full-length *TIAM1* isoform 1 and is defined as the reference here. *TIAM1* variants were generated by Q5 site-directed mutagenesis (New England Biolabs). Primers for mutagenesis are listed in Table S2. All the human cDNAs were cloned into pGW-UAS-HA.attB plasmid transgenic vector[35] and Sanger validated. The vectors were inserted into the VK37 (BDSC #24872) docking site by φC31-mediated transgenesis.[36]

Immunostaining

Immunostaining of fly larval and adult brains was performed as described.[37] Briefly, the dissected samples were fixed with 4% paraformaldehyde (PFA) in phosphate-buffered saline (PBS) followed by blocking in 0.2% PBS Triton X-100 (PBST) with 5% normal goat serum. Primary antibodies used were rat anti-*Drosophila* Elav (DSHB: 7E8A10) 1:500 and mouse anti-*Drosophila* Repo (DSHB: 8D12) 1:50. Secondary antibodies used were goat anti-rat-647 (Jackson ImmunoResearch, 112-605-003) 1:1,000 and goat anti-mouse-488 (Jackson ImmunoResearch, 115-545-062) 1:1,000. Samples were washed three times for 15 min with 0.2% PBST and mounted on a glass slide using Fluoromount-G (SouthernBiotech, 0100-20). Confocal microscopy (Zeiss LSM 880) was used for sample scanning, and images were processed using ImageJ.

Table 1. Clinical features of affected individuals with *TIAM1* variants

	Proband 1	MZ twin of proband 1	Proband 2	Proband 3	Proband 4
TIAM1 variant (GenBank: NM_001353694.2)	c.67C>T (p.Arg23Cys); c.2584C>T (p.Leu862Phe)	c.67C>T (p.Arg23Cys); c.2584C>T (p.Leu862Phe)	c.983G>T (p.Gly328Val)	c.4640C>A (p.Ala1547Glu)	c.1144G>C (p.Gly382Arg); c.4016C>T (p.Ala1339Val)
Genomic DNA, GRCh38	21:31266906 G>A; 21:31187079 G>A	21:31266906 G>A; 21:31187079 G>A	21:31252170 C>A	21:31120504 G>T	21:31252009 C>G; 21:31130242 G>A
CADD score	29.1; 23.7	29.1; 23.7	25.4	18.1	23.9; 26.7
Allele frequency (gnomAD)	4.04e−4; 3.98e−6	4.04e−4; 3.98e−6	8.18e−6	0	5.66e−5; 3.98e−6
Zygosity	compound heterozygous	compound heterozygous	homozygous	homozygous	compound heterozygous
Sex	M	M	M	M	F
Current age	35 years	35 years	3 years	7 years	6 years
Developmental delay	+	+	+	+	+
Intellectual disability	+	+	N/A	+ (severe)	+ (severe)
Delayed speech	+	+	+	+ (non-verbal)	+ (severe)
Autism	+	+	N/A	N/A	N/A
ADD/ADHD	+	+	N/A	N/A	N/A
Seizures	+	+	+, complex febrile seizures (abnormal EEGs)	+	+ (severe)
Brain MRI	N/A	N/A	progressive macrocephaly (secondary to chronic subdural hematoma and extra-axial fluid)	diffuse cerebral atrophy; thin corpus callosum; hypomyelination; deep cortical sulcus	hypothalamic hamartoma
Other neurological symptoms	none	impulsive, obsessive behavior	axial hypotonia; appendicular hypertonia	none	N/A
Endocrine symptoms	hypothyroidism; Addison's disease	hypothyroidism	subclinical hypothyroidism	hypomagnesemia	N/A
Other	none	none	dysmorphic features; congenital heart defect (atrial and ventricular septal defects); undescended testes	poor growth (difficulty in gaining weight); undescended testis; hirsutism	none
Consanguinity	none	none	+	+	none

MZ, monozygotic; CADD, combined annotation dependent depletion; M, male; N/A, not available; ADD, attention deficit disorder; ADHD, attention deficit hyperactivity disorder; EEG, electroencephalography.

Real-time PCR

Real-time PCR was performed as previously described[28] with the following changes: All-In-One 5X RT MasterMix (abm, G592), iTaq Universal SYBR Green Master Mix (BioRad, 1725120), and a BioRad C1000 Touch Cycler were used. Primers are listed in Table S2.

Statistical analysis

Statistical analysis was performed using GraphPad software (GraphPad Prism v9.0; GraphPad Software, USA). The statistical analyses of the lifespan assay were with log-rank (Mantel-Cox) and Gehan-Breslow-Wilcoxon tests, and analyses of the other assays were with two-tailed unpaired t tests. Data are represented as mean ± SEM, and n.s. (no significance) indicates $p > 0.05$; * $p < 0.05$; ** $p < 0.01$; *** $p < 0.001$; **** $p < 0.0001$.

Results

Summary of clinical findings

The affected individuals all have neurodevelopmental symptoms, mainly developmental delay, intellectual disability, speech delay, and seizures, and some have autism (supplemental note provides a summary of the clinical data). We first identified MZ twins similarly affected with these phenotypes carrying bi-allelic missense variants in *TIAM1* (proband 1). Using GeneMatcher,[38] we identified three other individuals with rare bi-allelic missense variants in *TIAM1*. Comprehensive clinical information including nucleotide changes and pedigrees can be found in Table 1, Figure S1, and supplemental note.

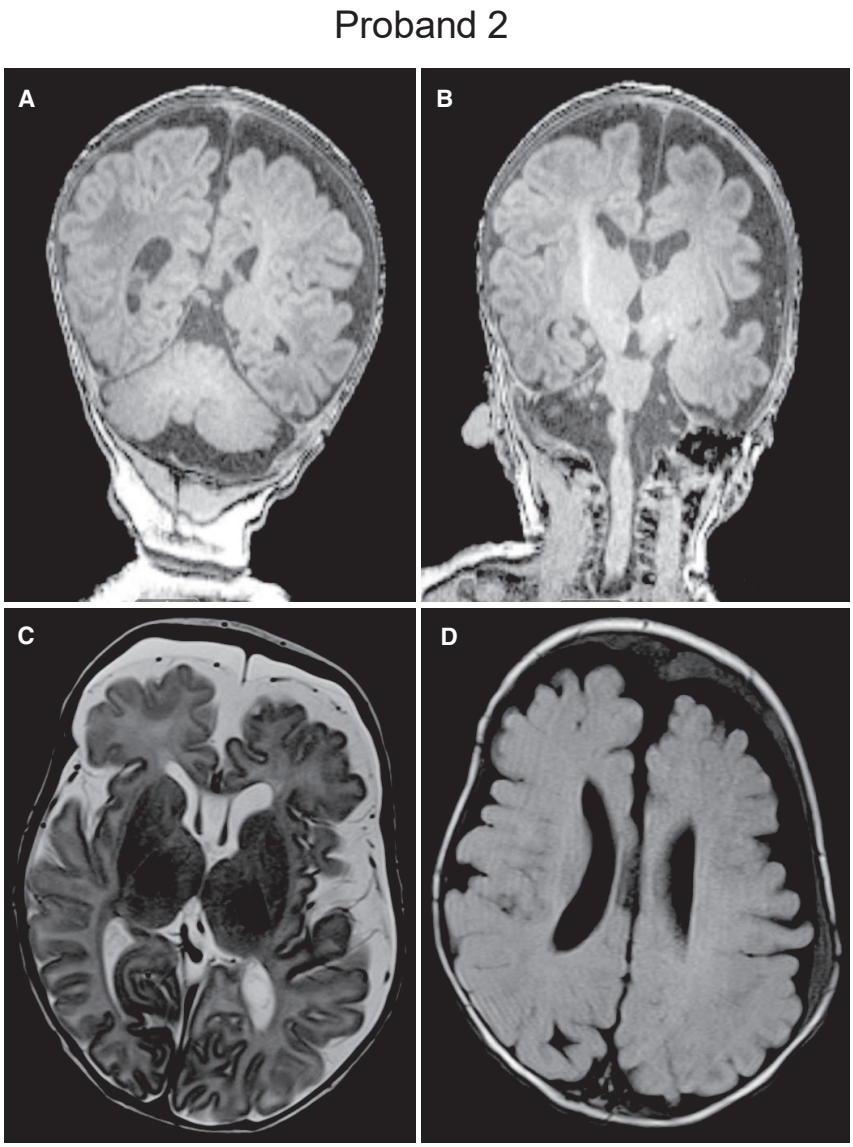

Figure 1. Brain MRI images of proband 2
(A–D) Brain MRI for proband 2 was obtained to document the acquired macrocephaly ($Z \geq 2$) at 14 months of age. 3T coronal T1 images (A and B) show prominence of the extra-axial fluid spaces involving both hemispheres, left greater than right, with prominence of the cortical sulci for age, enlargement of the lateral and third ventricles, and cavum septum pellucidum and cavum vergae. The brain parenchyma items show preservation of the gray-white matter differentiation with a myelination pattern appropriate for age. Axial T2 (C) and T2 FLAIR (D) images demonstrate intact and symmetric subcortical structures without evidence of heterotopia or other migrational defects. Also visible are prominent subarachnoid spaces with superimposed subdural collections most consistent on susceptibility-weighted imaging (not shown) as chronic subdural hemorrhage.

All probands are currently between the ages of 3 and 35 years. In two families (probands 2 and 3), the parents are consanguineous. All probands have neurodevelopmental disabilities with deficits especially noted in speech, including two probands who are non-verbal at 7 years of age. Seizures were reported in five individuals, with onset ranging from 2 months to 13 years of age. Three of the five individuals have abnormal brain MRIs, but the abnormalities are not consistent. Among them, proband 2 exhibited progressive macrocephaly thought to be secondary to chronic subdural hematoma or extra-axial fluid and diffuse cerebral atrophy (Figure 1), but it is unclear if these MRI features are primary to the condition or potentially due to another cause. Proband 2 had additional rare *de novo* or homozygous variants in *ALX4* (MIM: 605420) and *CYP27B1* (MIM: 609506), respectively, and proband 3 had rare homozygous variants in *PNLIP* (MIM: 246600), *SP4* (MIM: 600540), *WDR75*, and *ZGRF1* (Table S3), but none of these genes is known to contribute to the brain anatomy or neurocognition.

Other medical features observed in one or two probands include hypothyroidism, Addison's disease, congenital heart disease with septal defects, hypomagnesemia, and difficulty in gaining weight. Hypothyroidism was diagnosed in both MZ twins and required treatment with Synthroid, while an unrelated proband was found to have subclinical hypothyroidism.

To gather information about the variants, we queried MARRVEL (model organism aggregated resources for rare variant exploration, a resource for investigating human gene variants and model organism information).[10] The LoF observed/expected (o/e) score for *TIAM1* is 0.20, and the probability of being loss-of-function intolerant (pLI) score is 0.96, suggesting that *TIAM1* is intolerant to LoF alleles.[39] By querying the allele frequency in the Genome Aggregation Database (gnomAD),[39] the p.Ala1547Glu (c.4640C>A) variant is absent, while the p.Leu862Phe (c.2584C>T), p.Gly328Val (c.983G>T), p.Gly382Arg (c.1144G>C), and p.Ala1339Val (c.4016C>T) variants are observed in heterozygous individuals at extremely low frequencies (minor allele frequency [MAF] < 0.00006). The p.Arg23Cys (c.67C>T) variant is carried by heterozygous individuals at low frequency (MAF < 0.0005) based on gnomAD. Five of the six variants have combined annotation-dependent depletion (CADD)[40,41] scores higher than 20 (Table 1). Taken together, these variants with rare frequencies are likely to be disruptive.

sif is the *TIAM1* ortholog of *Drosophila*

To assess the impact of the *TIAM1* variants *in vivo*, we pursued experiments in *Drosophila*. The fly ortholog of *TIAM1*

A Prediction of *sif* human homologs

Fly Gene	Human Gene	DIOPT Score	Best Score	Best Score Reverse
sif	*TIAM1*	11	Yes	Yes
sif	*TIAM2*	8	No	Yes

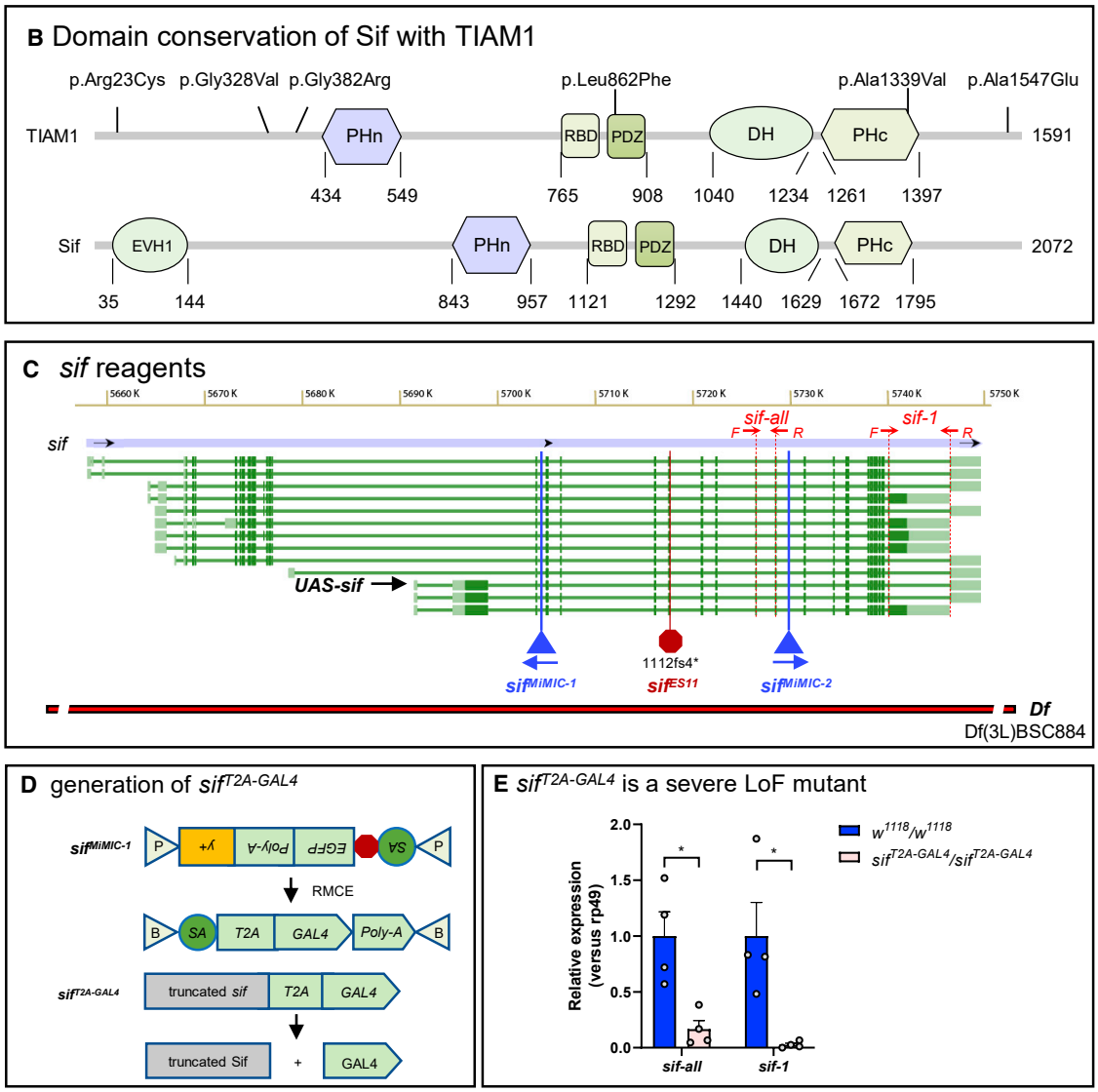

Figure 2. ***sif* is the *TIAM1* ortholog in fly**

(A) Prediction of *sif* human homologs using DIOPT (DRSC integrative ortholog prediction tool).

(B) Protein domain structure of TIAM1 and Sif.

(C) Genomic structure of *sif* locus and reagents used in this study. For detailed information on these reagents, please see Tables S1 and S2.

(D) Schematic of $sif^{T2A\text{-}GAL4}$ generation by RMCE using $sif^{MiMIC\text{-}1}$ ($sif^{MI02376}$, BDSC #35834). SA, splice acceptor; P, attP; B, attB; *y+*, *yellow+* gene as a marker.

(E) Relative *sif* mRNA expression levels are lower than 20% in $sif^{T2A\text{-}GAL4}$ mutant larvae when compared to controls (w^{1118}) based on real-time PCR using primers shown in (C). "*sif-all*" targets all of the 13 *sif* transcripts, while "*sif-1*" targets 8 of the 13 transcripts (*sif-RA*, *RB*, *RC*, *RI*, *RL*, *RM*, *RN*, and *RO*).

Each sample contains 3–5 L3 larvae. Data are represented as mean ± SEM. Unpaired t tests. *$p < 0.05$.

is *sif* with a DIOPT (DRSC integrative ortholog prediction tool) score of 11/16.[17] *sif* is also the ortholog of *TIAM2* (MIM: 604709) with a DIOPT score of 8/16[17] (Figure 2A). Sif and TIAM1 share 31% identity and 46% similarity,[17] and nearly all protein domains are shared between the two proteins (Figure 2B). In addition, three of the six *TIAM1* variants carried by the probands affect conserved amino acid residues (Figure S2).

The available *sif* reagents and tools are shown (Figure 2C and Table S1). They include $sif^{MiMIC\text{-}1}$, a MiMIC insertion in an early intron shared by all transcripts. MiMICs[24,26,42] allow us to replace the content between

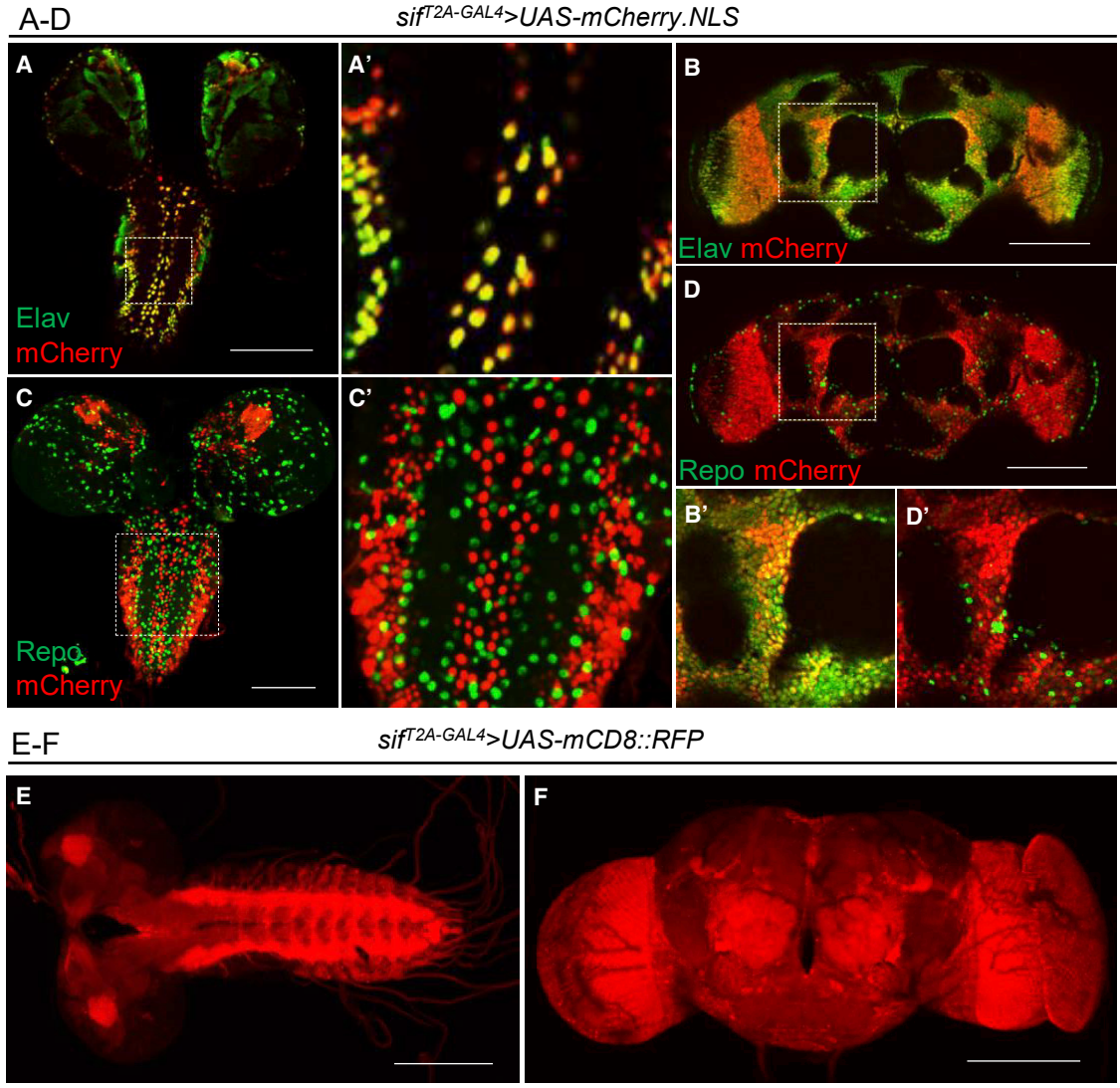

Figure 3. ***sif*** **is expressed primarily in neurons of the fly CNS**
(A–D) The L3 larval CNS (A, C) and adult brains (B, D) of $sif^{T2A\text{-}GAL4}$ allele-driven expression of *UAS-mCherry.NLS* (nuclear mCherry) were stained with markers for neurons (Elav, A and B) or glia (Repo, C and D). Single-slice confocal images are shown. (A′–D′) Images are from dashed squares of indicated regions to visualize the cellular co-localizations with Elav (A′ and B′) or Repo (C′ and D′). Scale bars: 100 μm. Note that *sif* is expressed in neurons.
(E and F) The $sif^{T2A\text{-}GAL4}$ allele-driven expression of *UAS-mCD8::RFP* (membrane-bound RFP) shows that *sif* is broadly detected in the CNS of L3 larvae (E) and adult flies (F). Scale bars: 100 μm.

the *attP* sites with the *splice acceptor (SA)-T2A-GAL4-polyA (T2A-GAL4)* cassette[43] via recombination-mediated cass ette exchange (RMCE)[25,42] (Figure 2D). The $sif^{T2A\text{-}GAL4}$ allele is predicted to be a null allele or severe LoF allele because the splice acceptor allows the artificial exon to be integrated into the mRNA, and the presence of the poly(A) tail leads to early transcription termination.[43] Based on real-time PCR, the total *sif* transcript levels are severely decreased when compared to wild-type (WT) control levels (w^{1118}) (Figure 2E). Furthermore, the viral T2A sequence allows ribosomal skipping and re-initiation of translation to produce GAL4[44] (Figure 2D). The GAL4 protein is therefore produced under the endogenous *sif* regulatory elements, and the $sif^{T2A\text{-}GAL4}$ allele allows us to drive expression of any *UAS-cDNA* in the same spatial and temporal pattern as the *sif* gene. The cDNA can be a fluorescent protein-encoding gene to reflect the endogenous expression, a human reference, or proband-specific cDNA to compare rescue ability of the $sif^{T2A\text{-}GAL4}$ mutants and assess if variants carried by the probands affect the protein function.[43,45,46]

sif is expressed primarily in neurons of the fly CNS

Given that the probands carrying *TIAM1* variants have neurological defects and *TIAM1* is enriched in the mammalian brain,[7] we explored the expression pattern of *sif* in the fly CNS. To determine the expression pattern, we crossed the $sif^{T2A\text{-}GAL4}$ mutants to *UAS-mCherry.NLS* (nuclear localized mCherry fluorescent protein) to label the nuclei of the cells that express *sif*. By co-staining

with the nuclear pan-neuronal marker Elav or nuclear pan-glial marker Repo, we found that mCherry (*sif*) is colocalized with a subset of Elav signals in the developing larval (Figure 3A) and adult CNS (Figure 3B). There is no obvious overlap of mCherry and Repo (glia) in both larval (Figures 3C) and adult brains (Figure 3D). The data are in agreement with the single-cell transcriptome atlas, SCope.[47,48] These data indicate that *sif* is mainly expressed in a subset of neurons but not in glia. To reveal the projections of cells that express *sif*, we used the $sif^{T2A\text{-}GAL4}$ allele to express *UAS-mCD8::RFP* (membrane-bound red fluorescent protein). As shown in Figure 3E, third instar larvae exhibit *sif* expression in the neuropil of the CNS, especially in the central brain and ventral nerve cord. In the adults, *sif* is enriched in the optic lobe, antennal lobe, and other brain regions (Figure 3F). The expression pattern of *sif* in the CNS suggested that *sif* may play a role during development and in adult stages.

Loss of *sif* impairs viability, and the surviving flies exhibit climbing defects and seizure-like behaviors

To investigate loss of *sif* phenotypes in flies, we assessed the survival rate associated with different *sif* LoF mutant flies. These include a sif^{ES11} allele,[19] a truncating *sif* allele induced by ethyl methanesulfonate; $sif^{MiMIC\text{-}2}$ ($Mi\{MIC\}sif^{MI07526}$), a MiMIC inserted in a late common intron of *sif* transcripts;[42] and a deletion that lacks *sif*, *Df(3L)BSC884* (*Df*). Based on complementation tests shown in Figure 4A, the $sif^{T2A\text{-}GAL4}$ allele is the most severe LoF allele if not a null allele. The $sif^{T2A\text{-}GAL4}$ allele causes semi-lethality, as only ~28% of the homozygous mutants eclose. The surviving adult flies exhibit very severe climbing defects. A similar number of survivors are observed in *trans*-heterozygous flies ($sif^{T2A\text{-}GAL4}/Df$) that also exhibit severe climbing defects when they are 3–5 days old (Figures 4A and 4B and Video S1). The $sif^{T2A\text{-}GAL4}$ chromosome is unlikely to carry second-site mutations that affect the survival rate, as the survival rates of $sif^{T2A\text{-}GAL4}/Df$ and $sif^{T2A\text{-}GAL4}/sif^{T2A\text{-}GAL4}$ are comparable, and both are fully rescued by *UAS-sif* fly cDNA expression[19] (see below). While sif^{ES11}/Df flies do not display decreased viability, they do exhibit severe climbing defects (Figure 4A). Finally, $sif^{MiMIC\text{-}2}/Df$ flies are viable and exhibit mild climbing defects (Figure 4A). Therefore, the lethality associated with sif^{ES11} and $sif^{MiMIC\text{-}2}$ homozygotes is likely caused by second-site mutations, and these alleles are hypomorphic for *sif*. These data suggest the allelic series from most severe to less severe is $sif^{T2A\text{-}GAL4} > sif^{ES11} > sif^{MiMIC\text{-}2}$. Note that the climbing defects are significantly rescued in the $sif^{T2A\text{-}GAL4}/Df$ flies when GAL4 drives *UAS-sif* expression (Figure 4B).

Given that the four probands exhibit seizures, we employed well-established protocols to induce seizure-like behaviors in *sif* LoF mutants. A seizure is a burst of uncontrolled electrical activity that causes abnormalities in muscle tone and even loss of consciousness. Owing to the similarities at the cellular and subcellular levels between fly and mammalian nervous systems, the fly has been used as a model for human seizures, or epilepsy.[49] Seizure-like behaviors in flies are characterized by aberrant posture with wing fluttering, leg twitching, and abdominal muscle contraction.[50–52] Seizures can be induced by mechanical stimulation[31] or hyperthermia.[32,53] The *sif* LoF mutants ($sif^{T2A\text{-}GAL4}/Df$ and $sif^{T2A\text{-}GAL4}/sif^{ES11}$) are extremely sensitive to seizures, as just a few knockdowns of vials containing these flies led to aberrant posture, wing fluttering, and leg twitching in 20%–30% of the flies (Video S1). We therefore tested the flies in a bang-sensitivity assay as well as heat-induced seizure assay. *sif* LoF mutants ($sif^{T2A\text{-}GAL4}/Df$) show a severe bang-sensitive phenotype and are slow to recover to an upright position after vortexing for 10 s (Figure 4C). Similarly, ~88% of the mutants show seizure-like behaviors when shifted from room temperature to 42°C for 30 s (Figure 4D), and they require more than 20 s on average to recover to an upright posture (Figure 4E). Again, the seizure-like behaviors are partially but significantly rescued by *UAS-sif* expression in $sif^{T2A\text{-}GAL4}/Df$ flies (Figures 4C–4E), showing that the phenotype is specifically due to loss of *sif* activity.

Climbing defects and seizure-like behaviors associated with *sif* LoF are mainly caused by neuronal loss of *sif*

To investigate the role of *sif* in different cell types, we tested climbing behaviors and seizure-like behaviors using *sif* RNAi lines driven by tissue-specific GAL4s. Two RNAi lines were used, *sif RNAi-1* and *sif RNAi-2* (Table S1). When driven by ubiquitous *daughterless-GAL4* (*da-GAL4*), the *sif* mRNA levels decreased by ~88% and ~76%, respectively (Figure 5A). Interestingly, *da-GAL4*-driven *UAS-* (*da >*) *sif RNAi-1* cause semi-lethality with a severe drop in survival rate to ~40% when compared to control flies (*da > luciferase RNAi*), whereas *da > sif RNAi-2* flies are fully viable (Figure 5B). The *da > sif RNAi-1 and sif RNAi-2* flies show climbing defects and seizure-like behaviors (Figures 5C–5E and Video S2). *da > sif RNAi-1* flies are more severely affected than *da > sif RNAi-2*, again highlighting a critical role for *sif* dosage. Since *sif* is highly enriched in neurons rather than glia in the CNS, we next used neuronal-specific *elav-GAL4* to knockdown *sif* in neurons.[54] Neuronal *sif* knockdowns show phenotypes similar to ubiquitous knockdowns (Figures 5F–5H and Video S3). We also tested glial knockdown of *sif* using *repo-GAL4* as controls: these flies do not show climbing defects (Figure 5I). Together, these data show that the neurological phenotypes, including climbing defects and seizure-like behaviors, of *sif* LoF mutants are mainly caused by neuronal loss of *sif*.

Human *TIAM1* Ref partially rescues the semi-lethality caused by *sif* loss, whereas the variants cause a variable rescue

To test whether human *TIAM1* can functionally replace the loss of *sif*, we first examined whether expression of the *TIAM1* Ref cDNA rescues the phenotypes of *sif* LoF mutants. We generated *UAS-TIAM1* cDNA transgenic fly lines expressing human *TIAM1* Ref, crossed the *UAS-TIAM1*

A Complementation tests

	$sif^{T2A\text{-}GAL4}$	sif^{ES11}	*Df(3L)BSC884*	$sif^{MiMIC\text{-}2}$
$sif^{T2A\text{-}GAL4}$	Semi-lethal‡ (28.3%)			
sif^{ES11}	Viable‡	Lethal		
Df(3L)BSC884	Semi-lethal‡ (32.8%)	Viable‡	Lethal	
$sif^{MiMIC\text{-}2}$	Viable#	Viable#	Viable#	Lethal

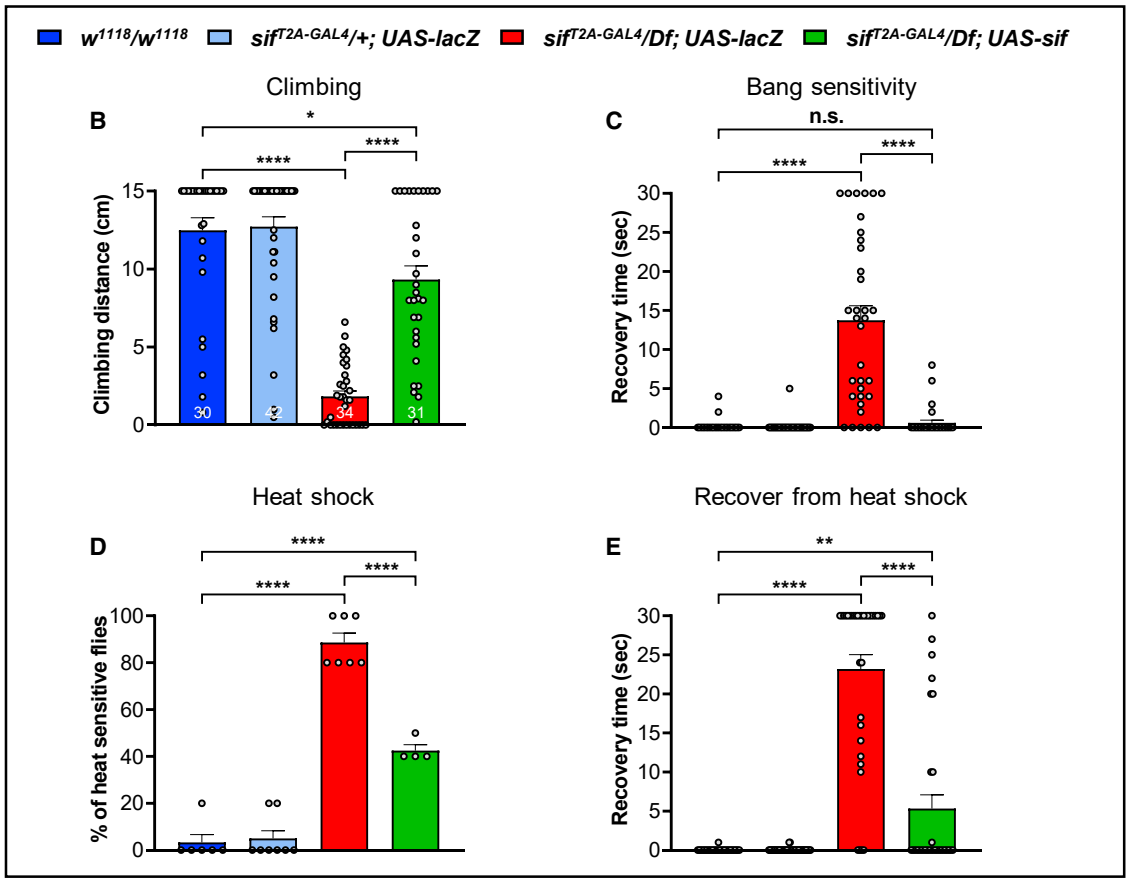

Figure 4. Loss of *sif* causes semi-lethality, and the surviving flies exhibit climbing defects and seizure-like behaviors
(A) Table summarizing complementation tests of *sif* LoF mutants. *sif* LoF mutants are semi-lethal and have severe ("‡") or mild ("#") climbing defects. The lethality of "sif^{ES11}" and "$sif^{MiMIC\text{-}2}$" homozygotes is likely caused by second-site mutations.
(B) *sif* LoF mutants have severe climbing defects 3–5 days after eclosion. Flies were raised at 22°C.
(C) *sif* LoF mutants have a bang-sensitive phenotype, which can be rescued by *UAS-sif* expression.
Flies were raised at 22°C and tested at day 3–5.
(D and E) *sif* LoF mutants have heat-induced seizure-like behaviors. Flies in vials were immersed in a 42°C water bath for 30 s. The percentage of flies that are unable to keep an upright position in *sif* LoF mutant group is significantly higher than the control groups (D), and the mutants could not recover 20 s after heat shock (E). The seizure-like behaviors can be rescued by *UAS-sif* expression.
Flies were raised at 22°C and tested at day 3–5. Data are represented as mean ± SEM. Unpaired t tests. *$p < 0.05$; **$p < 0.01$; ****$p < 0.0001$; n.s., no significance.

cDNA into the $sif^{T2A\text{-}GAL4}/Df$ background, and assessed survival rates. At 18°C, the *TIAM1* Ref can partially rescue the survival rate of $sif^{T2A\text{-}GAL4}/Df$, from 32.8% to 72.2% (Figure 6A). Since the GAL4 activity increases with temperature,[26,55] we also tested the rescue ability of *TIAM1* Ref at higher temperatures. However, the rescue ability of *TIAM1* Ref decreased to 26.0% at 22°C and 19.9% at 25°C, showing that overexpression of *TIAM1* is toxic (Figure 6A). Consistent with this interpretation, when we doubled the copy number of GAL4 at 18°C ($sif^{T2A\text{-}GAL4}/sif^{T2A\text{-}GAL4}$), the rescue ability of *TIAM1* Ref decreased from 72.2% to 42.1% (Figure 6B). These data indicate that *TIAM1* partially replaces the function of *sif*, but higher expression levels of *TIAM1* are toxic. Hence, the toxicity of *TIAM1* cDNA overexpression may limit its rescue ability. Furthermore, the *TIAM1* Ref and variants cannot rescue

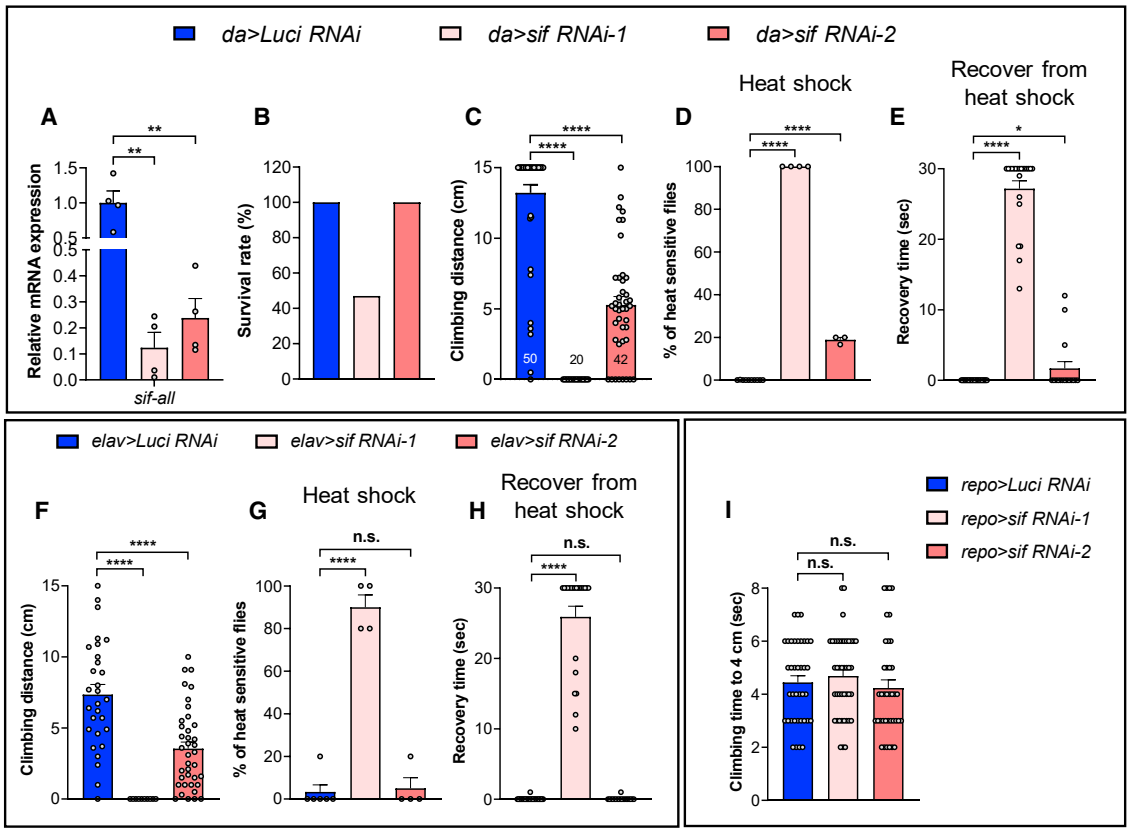

Figure 5. Neurological phenotypes of *sif* LoF mutants are mainly caused by neuronal loss of *sif*

(A) Real-time PCR analysis of *sif* mRNA levels in ubiquitous *sif* knockdown flies. Each sample contains 3–5 L3 larvae. *sif-RNAi-1* causes a higher knockdown efficiency than *sif-RNAi-2*.

(B) Survival rates of ubiquitous expression of *sif* RNAi at 25°C. *sif* knockdown with RNAi-1 causes semi-lethality, while RNAi-2 knockdown does not affect viability, indicating a strong dose dependency.

(C) Ubiquitous *sif* knockdown causes climbing defects in a dose-dependent manner. Flies were tested at day 3.

(D and E) Ubiquitous *sif* knockdown causes heat-induced seizure-like behaviors in a dose-dependent manner. The percentage of flies that are unable to keep an upright position in the *sif RNAi-1* group is significantly higher than controls (D), and the majority of flies are not able to recover 20 s after heat shock (E). Similar but milder phenotypes were seen in the *sif RNAi-2* group. Flies were tested at day 3.

(F) Neuronal *sif* knockdown causes climbing defects. Flies were allowed to climb for 5 s.

(G and H) Neuronal *sif* knockdown causes heat-induced seizures. The percentage of flies that are unable to keep an upright position in the *sif RNAi-1* group is significantly higher than controls (G), and the majority of flies in the *sif RNAi-1* group did not recover in 20 s after heat shock (H). Flies were tested at day 5.

(I) Glial *sif* knockdown does not cause climbing defects. Flies were tested at day 15.

All the animals were raised at 25°C unless otherwise mentioned. Data are represented as mean ± SEM. Unpaired t tests. *$p < 0.05$; **$p < 0.01$; ****$p < 0.0001$; n.s., no significance.

the neurological phenotypes associated with the *sif* LoF mutants (Figures S3A and S3B).

To investigate the rescue ability of the *TIAM1* variants observed in the probands, we generated *UAS-TIAM1* cDNA transgenic fly lines expressing human *TIAM1* variants in the $sif^{T2A\text{-}GAL4}/Df$ background. Since we did not obtain the variant information of proband 3 and 4 until late in the project, we only tested the three variants carried by probands 1 and 2. The *TIAM1* p.Arg23Cys variant shows significantly reduced survival rates when compared to *TIAM1* Ref (Figure 6B), suggesting that this is a partial LoF variant. The TIAM1 p.Leu862Phe and p.Gly328Val show survival rates comparable to those of the TIAM1 Ref, suggesting that they may be functional proteins. Similar rescue abilities were observed in the lifespan rescue assay (Figure 6C). However, since *TIAM1* overexpression is associated with toxicity, it is likely that there are two sources that reduce the viability in the rescue experiments: *sif* LoF and *TIAM1* cDNA overexpression. This affects the interpretation of the data. Since *TIAM1* Ref and variants may have different levels of toxicity upon overexpression, the rescue ability of the *TIAM1* cDNAs in *sif* LoF mutants may not be interpreted simply by viability. We therefore explored the function of *TIAM1* variants in a variety of overexpression assays in a WT background rather than in a LoF background (see below).

Ectopic expression of WT fly *sif* or human *TIAM1* Ref is toxic, and *TIAM1* variants are less toxic

Besides the LoF study, ectopic expression is also a useful tool to identify the function of a certain gene, since ectopic overexpression can sometimes induce phenotypes.[56,57] To further investigate the functional consequences of the

A

TIAM1 Ref partially rescues the viability of *sif* LoF mutants at 18 °C

Genotype		Survival rate		
		18 °C	22 °C	25 °C
$sif^{T2A\text{-}GAL4}$/Df; UAS-	*lacZ*	32.8%	31.0%	30.0%
	sif	102.0%	N/A	116.0%
	TIAM1 Ref	72.2%	26.0%	19.9%

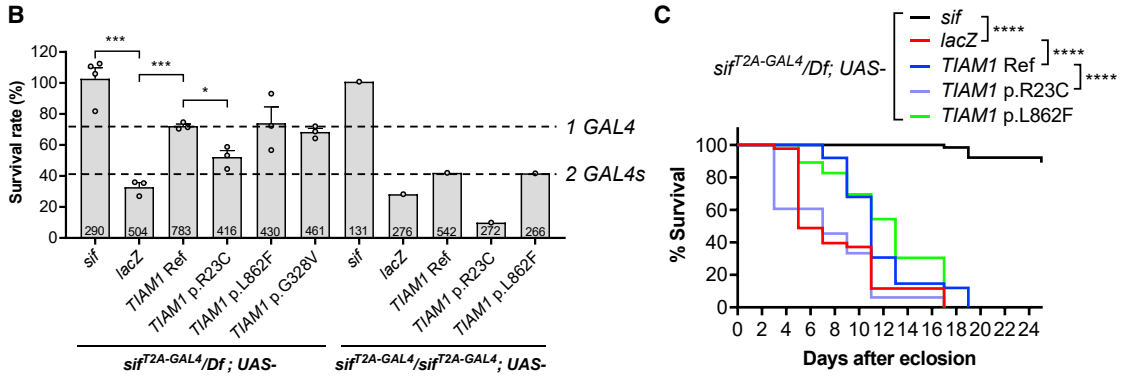

Figure 6. ***sif*** **LoF rescue studies show that** ***TIAM1*** **Ref has partial rescue ability, but the variants have variable rescue abilities**
(A) The rescue ability of *UAS-TIAM1* Ref decreases with increased temperature. *UAS-lacZ* was used as a negative control that doesn't alter the survival rate. Fly *UAS-sif* was used as a positive control, and it completely rescues the survival rate of *sif* LoF mutants.
(B) The semi-lethal phenotype of $sif^{T2A\text{-}GAL4}$ mutants can be fully rescued by expression of fly *sif* cDNA and partially rescued by *TIAM1* Ref cDNA. The TIAM1 variant p.Arg23Cys shows reduced rescue ability, while p.Leu862Phe and p.Gly328Val show similar rescue abilities when compared to TIAM1 Ref. Similar but lower rescue abilities were seen in $sif^{T2A\text{-}GAL4}$ homozygous background, suggesting two GAL4 copies cause higher *TIAM1*-induced toxicity. Flies were raised at 18°C.
(C) *sif* LoF mutants have significantly shorter lifespans, which can be rescued by *UAS-sif* and partially rescued by *UAS-TIAM1* Ref, while p.Arg23Cys shows reduced rescue ability. Flies were raised and kept at 18°C.
Data are represented as mean ± SEM. Unpaired t tests (B) and log-rank (Mantel-Cox) and Gehan-Breslow-Wilcoxon tests (C). *$p < 0.05$; ***$p < 0.001$; ****$p < 0.0001$; n.s., no significance.

TIAM1 variants, we overexpressed *UAS-TIAM1* in flies using various GAL4 drivers. We also used the *UAS-sif* transgenic flies for comparison.[19] Interestingly, ubiquitous overexpression of *sif* or *TIAM1* using *da-GAL4* causes lethality at 22°C and 25°C (Figure 7A, quantified in Figure 7B). Further, wing-specific overexpression of *sif* or *TIAM1* using *nub-GAL4* also causes a vein loss as well as blistery wings (Figure 7C, quantified in Figures S4A–S4C). These data indicate that *sif* and *TIAM1* are similarly toxic when overexpressed. We next tested whether the *TIAM1* variants alter the observed toxicity. We conducted these overexpression assays at different temperatures as this allows us to assess dose-dependent toxicity effects. At 18°C, the *da* > *TIAM1* Ref flies are viable, and there are no significant viability differences between *TIAM1* Ref and variants, suggesting that low expression levels of reference and variants are not or mildly toxic (Figure 7A). At 22°C, *da* > *TIAM1* Ref flies are L2 and L3 lethal. However, the surviving adult flies are observed with p.Leu862Phe, and a larger portion of animals survive into L3 stage carrying the p.Arg23Cys and p.Gly328Val variants than the Ref (Figure 7A, quantified in Figure 7B). At 25°C, *da* > *TIAM1* Ref flies are L2 lethal, but some pupae are observed in the p.Leu862Phe group (Figure 7A). Based on these experiments, the variants from most severe to least severe with respect to toxicity can be ordered as follows: TIAM1 Ref > p.Gly328Val > p.Arg23Cys > p.Leu862Phe (Figure 7B). These data are also consistent with the wing-specific expression assays as documented in Figure 7C and Figures S4A–S4C. It is worth noting that the survival rate of the wing-specific expression at 29°C corroborates the order of this allelic series as well (Figure S4D). Taken together, these ectopic overexpression studies support the hypothesis that p.Arg23Cys, p.Leu862Phe, and p.Gly328Val are partial LoF variants.

Discussion

Exome or genome sequencing of probands and parents with rare diseases combined with functional investigations in model organisms has led to the discovery of numerous novel Mendelian diseases.[2,4,58] Here, we identify *TIAM1* as a disease-associated gene. We present five individuals with compound-heterozygous or homozygous coding variants in *TIAM1*. The main phenotypes observed in the probands are developmental delays, with severe deficits in speech and language, intellectual disability, and seizures. Using *Drosophila*, we found that loss of *sif*, the ortholog of *TIAM1*, causes semi-lethality, and flies that eclose exhibit

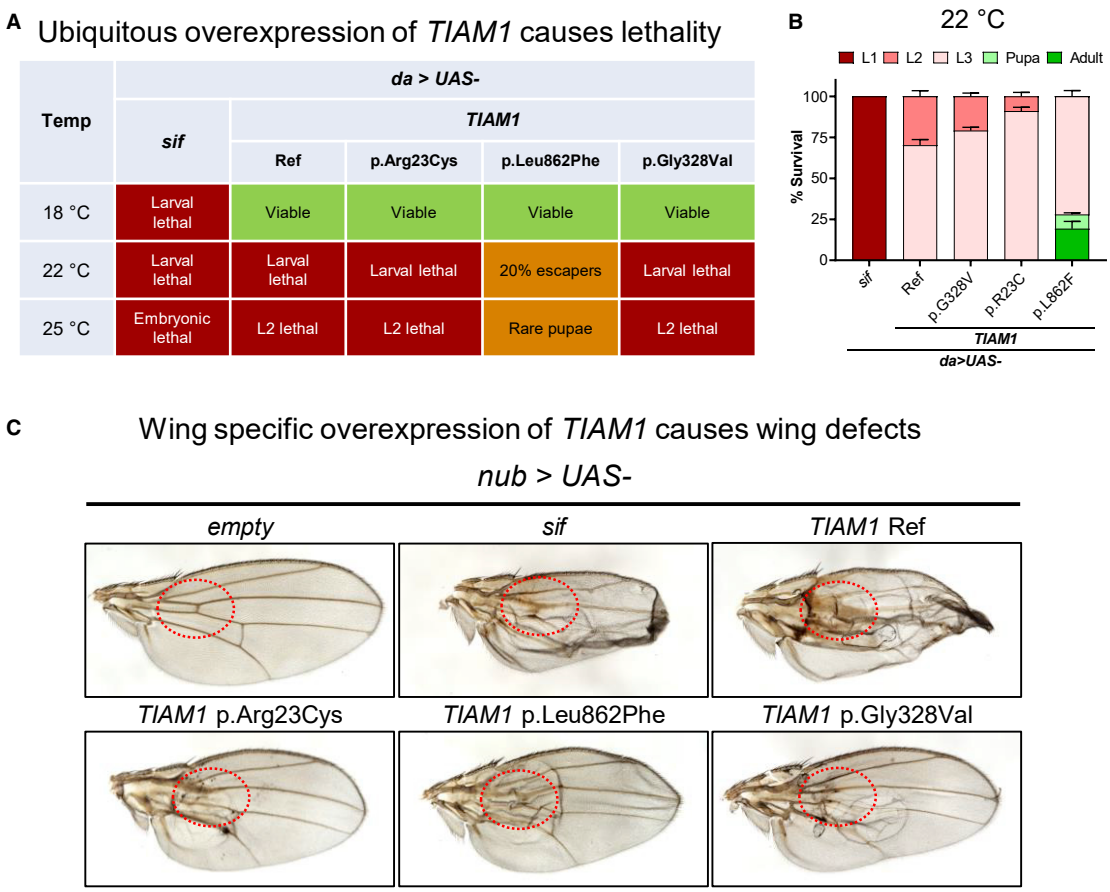

Figure 7. Ectopic expression of WT fly *sif* or human *TIAM1* Ref is toxic, but human *TIAM1* variants are less toxic
(A) Table summarizing the lethality phenotypes of ubiquitous overexpression (*da-GAL4*) of *sif*, *TIAM1* Ref, and variants.
(B) Quantification of survival stages of ubiquitous overexpression of *sif*, *TIAM1* Ref, and variants at 22°C. Note that the variants are less toxic. Data are represented as mean ± SEM.
(C) Representative pictures showing that wing-specific overexpression (*nub-GAL4*) of *sif* and *TIAM1* Ref causes similar vein loss and blistery wing phenotypes. The defects are highlighted in red dashed circles. Flies were raised and kept at 25°C.

climbing defects and seizure-like behaviors and have a short lifespan. The $sif^{T2A\text{-}GAL4}$ allele allowed us to determine the expression pattern of the gene and show that *sif* is expressed in neurons but not in glia. It also allowed us to "humanize" the fly by replacing fly *sif* with human *TIAM1*. We show that *TIAM1* Ref can partially rescue the survival rate and lifespan but not the climbing defects and seizure-like phenotypes of *sif* LoF mutants. The lack of rescue is likely due to the toxicity of the overexpression of *TIAM1* Ref in flies. Alternatively, the limited rescue ability is due to functional diversity of the human homologs, as there are four other orthologs of *sif* in humans besides *TIAM1*.[17]

The variant pathogenicity prediction algorithm CADD[41,59] indicates that these *TIAM1* variants are rare and likely pathogenic. Since the *TIAM1* variants carried by the probands reported here are bi-allelic, they are predicted to be LoF variants. To test this hypothesis, we assessed three of the six variants *in vivo* using two-pronged functional assays based on rescue and ectopic-expression experiments. We show that TIAM1 p.Arg23Cys has reduced rescue ability, suggesting that it is a partial LoF variant. TIAM1 p.Leu862Phe and p.Gly328Val show rescue ability comparable to that of TIAM1 Ref and did not allow us to draw a conclusion based on this assay, since *TIAM1* cDNAs have different levels of toxicity that also affect viability. Therefore, we used ectopic-expression experiments in a WT background to further test the function of the variants, given that WT *sif* and *TIAM1* Ref induce similar phenotypes, including wing defects, in ectopic-expression assays. Since *TIAM1* Ref and the variants are inserted in the same genomic site, we can perform functional analyses of the variants by comparing ectopic-expression-induced phenotypes. The three proband-associated variants exhibit reduced toxicity when compared to *TIAM1* Ref. When the Ref causes a toxic phenotype and the variants are less toxic, the variants can typically be classified as LoF variants.[1,33,60–64] Hence, our ectopic-expression data support the hypothesis that TIAM1 p.Arg23Cys, p.Leu862Phe, and p.Gly328Val are partial LoF variants. Taken together, our data suggest that the *TIAM1* variants reported here result in a loss of function and are associated with neurodevelopmental phenotypes and seizures.

The bioinformatic data show that the pLI of *TIAM1* is high (0.96), and the observed-to-expected ratio of LoF

variants for *TIAM1* is 0.20.[39] However, there are 46 heterozygous individuals with *TIAM1* LoF alleles observed in gnomAD, suggesting that loss of one copy of *TIAM1* is tolerated. A possible reason why *TIAM1* is associated with a high pLI score is that it is a very large gene (>400 kb). We previously also reported an autosomal-recessive disease associated with bi-allelic LoF variants in *OXR1*,[65] a large gene (>400 kb) for which the observed-to-expected ratio of LoF variants is 0.19 and the pLI is 0.84,[10] very similar to *TIAM1*.

Besides *TIAM1*, *sif* is also the ortholog of other GEF-encoding genes, including *TIAM2*, *DNMBP* (MIM: 611282), *ARHGEF37*, and *ARHGEF38*.[17] TIAM2 activates RAC1 and controls cell migration in neurons.[66] DNMBP is a GEF for cell division control protein 42 that controls the shaping of cell junctions through binding to tight junction protein ZO-1, and knockdown of *DNMBP* results in a disorganized configuration of cell junctions.[67] LoF variants of *DNMBP* cause infantile-onset cataracts in humans.[22] Similarly, *sif* knockdown in the eye alters the distribution of septate junctions in adjacent cone cells and affects the function of the eye in young flies.[22] Finally, ARHGEF37 and ARHGEF38 are Rho GEFs. ARHGEF37 assists dynamin 2 during clathrin-mediated endocytosis,[68] while ARHGEF38 is an uncharacterized protein.

Tiam1 knockout mice have decreased spine density, simplified dendritic arbors, and decreased miniature excitatory postsynaptic currents in the hippocampus, but they exhibit only subtle behavior abnormalities,[15] which may be due to redundancy of other GEFs. The related TIAM2 shares 37% overall identity and 71% Dbl homology (DH) domain identity with TIAM1.[69–71] The expression levels of *Tiam2* correlate with the stages of neuronal morphological development, and *Tiam2* knockdown in neurons also causes reduced neurite outgrowth.[72,73] TIAM1 promotes the formation and growth of spines and synapses by activating RAC1 signaling pathways that control the actin cytoskeleton. Dysfunction of the neuronal cytoskeleton has been implicated in a variety of diseases, including neurological developmental disorders as well as neurodegenerative diseases.[74,75] Moreover, dysregulation of the neuronal cytoskeletal network also contributes to the pathogenesis of epilepsy.[76–78]

Previous studies show that *sif* LoF mutants are viable and have reduced locomotor activity.[18,19] In this study, we generated a more severe LoF allele, $sif^{T2A\text{-}GAL4}$, which leads to semi-lethality, a highly reduced lifespan, and a severe sensitivity to seizure-like behaviors, in addition to the climbing defects. It is worth noting that fly mutants with such severe sensitivity to seizures are rarely observed.[60,61,79] We also show that these phenotypes are mainly caused by neuronal *sif* loss based on RNAi knockdown assays. Interestingly, the *sif RNAi-1* with ~12% of the remaining *sif* transcripts based on real-time PCR show much stronger phenotypes, including semi-lethality, when compared to *sif RNAi-2* with ~24% remaining *sif* transcripts, indicating a threshold effect of *sif* expression between these two values, similar to what has been documented for other genes, like *flower*.[80]

Finally, we would like to point out the limitations of our study. The number of individuals described is small and some of the phenotypic features differ. Two of the individuals come from consanguineous families, and additional recessive conditions could be contributing to the phenotype. Additionally, the analysis was based on exome sequencing, and noncoding variants were not assessed and could contribute to variation in the phenotype. With additional identified individuals with bi-allelic *TIAM1* variants, it should become more obvious which clinical features are core to the condition.

In summary, we find that bi-allelic pathogenic *TIAM1* variants are associated with a neurological disorder in humans. We provide functional analysis in flies that supports an LoF model for *TIAM1*-associated variants. Further studies of the underlying mechanism will be necessary to provide a better understanding of the pathological mechanisms and may provide therapeutic strategies.

Data and code availability

This study did not generate datasets. All reagents developed in this study are available upon request. There are restrictions to the availability of sequencing data of the research participants due to privacy and ethical/legal issues.

Supplemental information

Supplemental information can be found online at https://doi.org/10.1016/j.ajhg.2022.01.020.

Acknowledgments

We thank the probands and families for agreeing to participate in this study. We thank Dr. Xiao Mao for his effort in bringing us into contact with the clinicians and the family in China. We thank Dr. Sjoerd Verkaart for technical support. We thank former and present Bellen and Yamamoto lab members for their discussion and suggestions in this study, particularly Debdeep Dutta, Scott Barish, Mengqi Ma, and Yiming Zheng. We thank Ms. Hongling Pan for the injection of transgenic fly lines. We thank Dr. Michael Wangler for the guidelines for the IRB protocol. We thank the BDSC for numerous stocks. This work was supported by the Howard Hughes Medical Institute (HHMI), the Huffington Foundation, and the Jan and Dan Duncan Neurological Research Institute at Texas Children's Hospital to H.J.B. Research reported in this publication was also supported by the Eunice Kennedy Shriver National Institute of Child Health & Human Development of the National Institutes of Health (NIH) under award number P50HD103555 for use of the neurovisualization core facilities. The content is solely the responsibility of the authors and does not necessarily represent the official views of the NIH. Further support came from The Office of Research Infrastructure Programs of the NIH under the award numbers R24 OD022005 and R24 OD031447 to H.J.B. P.C.M. is supported by CIHR (MFE-164712) and the Stand by Eli Foundation. H.C. is supported by Warren Alpert Foundation.

Declaration of interests

M.J.G.S. is a salaried employee of GeneDx Inc.

Received: November 1, 2021
Accepted: January 27, 2022
Published: March 2, 2022

Web resources

CADD, https://cadd.gs.washington.edu/
DIOPT, https://www.flyrnai.org/cgi-bin/DRSC_orthologs.pl
GeneDx ClinVar submission page, https://www.ncbi.nlm.nih.gov/clinvar/submitters/26957/
GeneMatcher, https://genematcher.org/statistics/
gnomAD, https://gnomad.broadinstitute.org/
MARRVEL, http://www.marrvel.org/
OMIM, https://www.omim.org/

References

1. Splinter, K., Adams, D.R., Bacino, C.A., Bellen, H.J., Bernstein, J.A., Cheatle-Jarvela, A.M., Eng, C.M., Esteves, C., Gahl, W.A., Hamid, R., et al.; Undiagnosed Diseases Network (2018). Effect of Genetic Diagnosis on Patients with Previously Undiagnosed Disease. N. Engl. J. Med. *379*, 2131–2139. https://doi.org/10.1056/NEJMoa1714458.
2. Wangler, M.F., Yamamoto, S., Chao, H.T., Posey, J.E., Westerfield, M., Postlethwait, J., Hieter, P., Boycott, K.M., Campeau, P.M., Bellen, H.J.; and Members of the Undiagnosed Diseases Network (UDN) (2017). Model Organisms Facilitate Rare Disease Diagnosis and Therapeutic Research. Genetics *207*, 9–27. https://doi.org/10.1534/genetics.117.203067.
3. Coventry, A., Bull-Otterson, L.M., Liu, X., Clark, A.G., Maxwell, T.J., Crosby, J., Hixson, J.E., Rea, T.J., Muzny, D.M., Lewis, L.R., et al. (2010). Deep resequencing reveals excess rare recent variants consistent with explosive population growth. Nat. Commun. *1*, 131. https://doi.org/10.1038/ncomms1130.
4. Bellen, H.J., Wangler, M.F., and Yamamoto, S. (2019). The fruit fly at the interface of diagnosis and pathogenic mechanisms of rare and common human diseases. Hum. Mol. Genet. *28* (R2), R207–R214. https://doi.org/10.1093/hmg/ddz135.
5. Lambert, J.M., Lambert, Q.T., Reuther, G.W., Malliri, A., Siderovski, D.P., Sondek, J., Collard, J.G., and Der, C.J. (2002). Tiam1 mediates Ras activation of Rac by a PI(3)K-independent mechanism. Nat. Cell Biol. *4*, 621–625. https://doi.org/10.1038/ncb833.
6. Leeuwen, F.N., Kain, H.E., Kammen, R.A., Michiels, F., Kranenburg, O.W., and Collard, J.G. (1997). The guanine nucleotide exchange factor Tiam1 affects neuronal morphology; opposing roles for the small GTPases Rac and Rho. J. Cell Biol. *139*, 797–807. https://doi.org/10.1083/jcb.139.3.797.
7. Tolias, K.F., Bikoff, J.B., Burette, A., Paradis, S., Harrar, D., Tavazoie, S., Weinberg, R.J., and Greenberg, M.E. (2005). The Rac1-GEF Tiam1 couples the NMDA receptor to the activity-dependent development of dendritic arbors and spines. Neuron *45*, 525–538. https://doi.org/10.1016/j.neuron.2005.01.024.
8. Bos, J.L., Rehmann, H., and Wittinghofer, A. (2007). GEFs and GAPs: critical elements in the control of small G proteins. Cell *129*, 865–877. https://doi.org/10.1016/j.cell.2007.05.018.
9. Tolias, K.F., Bikoff, J.B., Kane, C.G., Tolias, C.S., Hu, L., and Greenberg, M.E. (2007). The Rac1 guanine nucleotide exchange factor Tiam1 mediates EphB receptor-dependent dendritic spine development. Proc. Natl. Acad. Sci. USA *104*, 7265–7270. https://doi.org/10.1073/pnas.0702044104.
10. Wang, J., Al-Ouran, R., Hu, Y., Kim, S.Y., Wan, Y.W., Wangler, M.F., Yamamoto, S., Chao, H.T., Comjean, A., Mohr, S.E., et al.; UDN (2017). MARRVEL: Integration of Human and Model Organism Genetic Resources to Facilitate Functional Annotation of the Human Genome. Am. J. Hum. Genet. *100*, 843–853. https://doi.org/10.1016/j.ajhg.2017.04.010.
11. Consortium, G.T.; and GTEx Consortium (2015). Human genomics. The Genotype-Tissue Expression (GTEx) pilot analysis: multitissue gene regulation in humans. Science *348*, 648–660. https://doi.org/10.1126/science.1262110.
12. Miyamoto, Y., Yamauchi, J., Tanoue, A., Wu, C., and Mobley, W.C. (2006). TrkB binds and tyrosine-phosphorylates Tiam1, leading to activation of Rac1 and induction of changes in cellular morphology. Proc. Natl. Acad. Sci. USA *103*, 10444–10449. https://doi.org/10.1073/pnas.0603914103.
13. Shirazi Fard, S., Kele, J., Vilar, M., Paratcha, G., and Ledda, F. (2010). Tiam1 as a signaling mediator of nerve growth factor-dependent neurite outgrowth. PLoS ONE *5*, e9647. https://doi.org/10.1371/journal.pone.0009647.
14. Zhang, H., and Macara, I.G. (2006). The polarity protein PAR-3 and TIAM1 cooperate in dendritic spine morphogenesis. Nat. Cell Biol. *8*, 227–237. https://doi.org/10.1038/ncb1368.
15. Cheng, J., Scala, F., Blanco, F.A., Niu, S., Firozi, K., Keehan, L., Mulherkar, S., Froudarakis, E., Li, L., Duman, J.G., et al. (2021). The Rac-GEF Tiam1 Promotes Dendrite and Synapse Stabilization of Dentate Granule Cells and Restricts Hippocampal-Dependent Memory Functions. J. Neurosci. *41*, 1191–1206. https://doi.org/10.1523/JNEUROSCI.3271-17.2020.
16. Amberger, J.S., Bocchini, C.A., Schiettecatte, F., Scott, A.F., and Hamosh, A. (2015). OMIM.org: Online Mendelian Inheritance in Man (OMIM®), an online catalog of human genes and genetic disorders. Nucleic Acids Res. *43*, D789–D798. https://doi.org/10.1093/nar/gku1205.
17. Hu, Y., Flockhart, I., Vinayagam, A., Bergwitz, C., Berger, B., Perrimon, N., and Mohr, S.E. (2011). An integrative approach to ortholog prediction for disease-focused and other functional studies. BMC Bioinformatics *12*, 357. https://doi.org/10.1186/1471-2105-12-357.
18. Sone, M., Hoshino, M., Suzuki, E., Kuroda, S., Kaibuchi, K., Nakagoshi, H., Saigo, K., Nabeshima, Y., and Hama, C. (1997). Still life, a protein in synaptic terminals of Drosophila homologous to GDP-GTP exchangers. Science *275*, 543–547. https://doi.org/10.1126/science.275.5299.543.
19. Sone, M., Suzuki, E., Hoshino, M., Hou, D., Kuromi, H., Fukata, M., Kuroda, S., Kaibuchi, K., Nabeshima, Y., and Hama, C. (2000). Synaptic development is controlled in the periactive zones of Drosophila synapses. Development *127*, 4157–4168.
20. Schuster, C.M., Davis, G.W., Fetter, R.D., and Goodman, C.S. (1996). Genetic dissection of structural and functional components of synaptic plasticity. II. Fasciclin II controls presynaptic structural plasticity. Neuron *17*, 655–667. https://doi.org/10.1016/s0896-6273(00)80198-1.
21. Schuster, C.M., Davis, G.W., Fetter, R.D., and Goodman, C.S. (1996). Genetic dissection of structural and functional components of synaptic plasticity. I. Fasciclin II controls synaptic

stabilization and growth. Neuron *17*, 641–654. https://doi.org/10.1016/s0896-6273(00)80197-x.

22. Ansar, M., Chung, H.L., Taylor, R.L., Nazir, A., Imtiaz, S., Sarwar, M.T., Manousopoulou, A., Makrythanasis, P., Saeed, S., Falconnet, E., et al. (2018). Bi-allelic Loss-of-Function Variants in DNMBP Cause Infantile Cataracts. Am. J. Hum. Genet. *103*, 568–578. https://doi.org/10.1016/j.ajhg.2018.09.004.
23. Retterer, K., Juusola, J., Cho, M.T., Vitazka, P., Millan, F., Gibellini, F., Vertino-Bell, A., Smaoui, N., Neidich, J., Monaghan, K.G., et al. (2016). Clinical application of whole-exome sequencing across clinical indications. Genet. Med. *18*, 696–704. https://doi.org/10.1038/gim.2015.148.
24. Venken, K.J., Schulze, K.L., Haelterman, N.A., Pan, H., He, Y., Evans-Holm, M., Carlson, J.W., Levis, R.W., Spradling, A.C., Hoskins, R.A., and Bellen, H.J. (2011). MiMIC: a highly versatile transposon insertion resource for engineering Drosophila melanogaster genes. Nat. Methods *8*, 737–743. https://doi.org/10.1038/nmeth.1662.
25. Diao, F., Ironfield, H., Luan, H., Diao, F., Shropshire, W.C., Ewer, J., Marr, E., Potter, C.J., Landgraf, M., and White, B.H. (2015). Plug-and-play genetic access to drosophila cell types using exchangeable exon cassettes. Cell Rep. *10*, 1410–1421. https://doi.org/10.1016/j.celrep.2015.01.059.
26. Nagarkar-Jaiswal, S., Lee, P.T., Campbell, M.E., Chen, K., Anguiano-Zarate, S., Gutierrez, M.C., Busby, T., Lin, W.W., He, Y., Schulze, K.L., et al. (2015). A library of MiMICs allows tagging of genes and reversible, spatial and temporal knockdown of proteins in Drosophila. eLife *4*. https://doi.org/10.7554/eLife.05338.
27. Yao, C.K., Lin, Y.Q., Ly, C.V., Ohyama, T., Haueter, C.M., Moiseenkova-Bell, V.Y., Wensel, T.G., and Bellen, H.J. (2009). A synaptic vesicle-associated Ca2+ channel promotes endocytosis and couples exocytosis to endocytosis. Cell *138*, 947–960. https://doi.org/10.1016/j.cell.2009.06.033.
28. Goodman, L.D., Cope, H., Nil, Z., Ravenscroft, T.A., Charng, W.L., Lu, S., Tien, A.C., Pfundt, R., Koolen, D.A., Haaxma, C.A., et al.; Undiagnosed Diseases Network (2021). TNPO2 variants associate with human developmental delays, neurologic deficits, and dysmorphic features and alter TNPO2 activity in Drosophila. Am. J. Hum. Genet. *108*, 1669–1691. https://doi.org/10.1016/j.ajhg.2021.06.019.
29. Madabattula, S.T., Strautman, J.C., Bysice, A.M., O'Sullivan, J.A., Androschuk, A., Rosenfelt, C., Doucet, K., Rouleau, G., and Bolduc, F. (2015). Quantitative Analysis of Climbing Defects in a Drosophila Model of Neurodegenerative Disorders. J. Vis. Exp. *52741*, e52741. https://doi.org/10.3791/52741.
30. Hatfield, I., Harvey, I., Yates, E.R., Redd, J.R., Reiter, L.T., and Bridges, D. (2015). The role of TORC1 in muscle development in Drosophila. Sci. Rep. *5*, 9676. https://doi.org/10.1038/srep09676.
31. Ganetzky, B., and Wu, C.F. (1982). Indirect Suppression Involving Behavioral Mutants with Altered Nerve Excitability in DROSOPHILA MELANOGASTER. Genetics *100*, 597–614.
32. Burg, M.G., and Wu, C.F. (2012). Mechanical and temperature stressor-induced seizure-and-paralysis behaviors in Drosophila bang-sensitive mutants. J. Neurogenet. *26*, 189–197. https://doi.org/10.3109/01677063.2012.690011.
33. Ansar, M., Chung, H.L., Al-Otaibi, A., Elagabani, M.N., Ravenscroft, T.A., Paracha, S.A., Scholz, R., Abdel Magid, T., Sarwar, M.T., Shah, S.F., et al. (2019). Bi-allelic Variants in IQSEC1 Cause Intellectual Disability, Developmental Delay, and Short Stature. Am. J. Hum. Genet. *105*, 907–920. https://doi.org/10.1016/j.ajhg.2019.09.013.
34. Harnish, J.M., Deal, S.L., Chao, H.T., Wangler, M.F., and Yamamoto, S. (2019). In Vivo Functional Study of Disease-associated Rare Human Variants Using Drosophila. J. Vis. Exp. (150) https://doi.org/10.3791/59658..
35. Bischof, J., Björklund, M., Furger, E., Schertel, C., Taipale, J., and Basler, K. (2013). A versatile platform for creating a comprehensive UAS-ORFeome library in Drosophila. Development *140*, 2434–2442. https://doi.org/10.1242/dev.088757.
36. Venken, K.J., He, Y., Hoskins, R.A., and Bellen, H.J. (2006). P [acman]: a BAC transgenic platform for targeted insertion of large DNA fragments in D. melanogaster. Science *314*, 1747–1751. https://doi.org/10.1126/science.1134426.
37. Dutta, D., Briere, L.C., Kanca, O., Marcogliese, P.C., Walker, M.A., High, F.A., Vanderver, A., Krier, J., Carmichael, N., Callahan, C., et al. (2020). De novo mutations in TOMM70, a receptor of the mitochondrial import translocase, cause neurological impairment. Hum. Mol. Genet. *29*, 1568–1579. https://doi.org/10.1093/hmg/ddaa081.
38. Sobreira, N., Schiettecatte, F., Valle, D., and Hamosh, A. (2015). GeneMatcher: a matching tool for connecting investigators with an interest in the same gene. Hum. Mutat. *36*, 928–930. https://doi.org/10.1002/humu.22844.
39. Karczewski, K.J., Francioli, L.C., Tiao, G., Cummings, B.B., Alföldi, J., Wang, Q., Collins, R.L., Laricchia, K.M., Ganna, A., Birnbaum, D.P., et al.; Genome Aggregation Database Consortium (2020). The mutational constraint spectrum quantified from variation in 141,456 humans. Nature *581*, 434–443. https://doi.org/10.1038/s41586-020-2308-7.
40. Rentzsch, P., Schubach, M., Shendure, J., and Kircher, M. (2021). CADD-Splice-improving genome-wide variant effect prediction using deep learning-derived splice scores. Genome Med. *13*, 31. https://doi.org/10.1186/s13073-021-00835-9.
41. Kircher, M., Witten, D.M., Jain, P., O'Roak, B.J., Cooper, G.M., and Shendure, J. (2014). A general framework for estimating the relative pathogenicity of human genetic variants. Nat. Genet. *46*, 310–315. https://doi.org/10.1038/ng.2892.
42. Nagarkar-Jaiswal, S., DeLuca, S.Z., Lee, P.T., Lin, W.W., Pan, H., Zuo, Z., Lv, J., Spradling, A.C., and Bellen, H.J. (2015). A genetic toolkit for tagging intronic MiMIC containing genes. eLife *4*. https://doi.org/10.7554/eLife.08469.
43. Lee, P.T., Zirin, J., Kanca, O., Lin, W.W., Schulze, K.L., Li-Kroeger, D., Tao, R., Devereaux, C., Hu, Y., Chung, V., et al. (2018). A gene-specific *T2A-GAL4* library for *Drosophila*. eLife *7*, e35574. https://doi.org/10.7554/eLife.35574.
44. Diao, F., and White, B.H. (2012). A novel approach for directing transgene expression in Drosophila: T2A-Gal4 in-frame fusion. Genetics *190*, 1139–1144. https://doi.org/10.1534/genetics.111.136291.
45. Chung, H.L., Wangler, M.F., Marcogliese, P.C., Jo, J., Ravenscroft, T.A., Zuo, Z., Duraine, L., Sadeghzadeh, S., Li-Kroeger, D., Schmidt, R.E., et al.; Members of Undiagnosed Diseases Network (2020). Loss- or Gain-of-Function Mutations in ACOX1 Cause Axonal Loss via Different Mechanisms. Neuron *106*, 589–606.e6. https://doi.org/10.1016/j.neuron.2020.02.021.
46. Marcogliese, P.C., Deal, S.L., Andrews, J., Harnish, J.M., Bhavana, V.H., Graves, H.K., Jangam, S., Luo, X., Liu, N., Bei, D., et al. (2021). *Drosophila* functional screening of *de novo* variants in autism uncovers deleterious variants and facilitates

discovery of rare neurodevelopmental diseases. Preprint at bioRxiv. https://doi.org/10.1101/2020.12.30.424813.
47. Davie, K., Janssens, J., Koldere, D., De Waegeneer, M., Pech, U., Kreft, Ł., Aibar, S., Makhzami, S., Christiaens, V., Bravo González-Blas, C., et al. (2018). A Single-Cell Transcriptome Atlas of the Aging Drosophila Brain. Cell *174*, 982–998.e20. https://doi.org/10.1016/j.cell.2018.05.057.
48. Li, H., Janssens, J., De Waegeneer, M., Kolluru, S.S., Davie, K., Gardeux, V., Saelens, W., David, F., Brbić, M., Leskovec, J., et al. (2021). Fly Cell Atlas: a single-cell transcriptomic atlas of the adult fruit fly. Preprint at bioRxiv. https://doi.org/10.1101/2021.07.04.451050.
49. Parker, L., Howlett, I.C., Rusan, Z.M., and Tanouye, M.A. (2011). Seizure and epilepsy: studies of seizure disorders in Drosophila. Int. Rev. Neurobiol. *99*, 1–21. https://doi.org/10.1016/B978-0-12-387003-2.00001-X.
50. Dare, S.S., Merlo, E., Rodriguez Curt, J., Ekanem, P.E., Hu, N., and Berni, J. (2021). *Drosophila para* ^{bss} Flies as a Screening Model for Traditional Medicine: Anticonvulsant Effects of *Annona senegalensis*. Front. Neurol. *11*, 606919. https://doi.org/10.3389/fneur.2020.606919.
51. Parker, L., Padilla, M., Du, Y., Dong, K., and Tanouye, M.A. (2011). Drosophila as a model for epilepsy: bss is a gain-of-function mutation in the para sodium channel gene that leads to seizures. Genetics *187*, 523–534. https://doi.org/10.1534/genetics.110.123299.
52. Saras, A., Wu, V.V., Brawer, H.J., and Tanouye, M.A. (2017). Investigation of Seizure-Susceptibility in a *Drosophila melanogaster* Model of Human Epilepsy with Optogenetic Stimulation. Genetics *206*, 1739–1746. https://doi.org/10.1534/genetics.116.194779.
53. Sun, L., Gilligan, J., Staber, C., Schutte, R.J., Nguyen, V., O'Dowd, D.K., and Reenan, R. (2012). A knock-in model of human epilepsy in Drosophila reveals a novel cellular mechanism associated with heat-induced seizure. J. Neurosci. *32*, 14145–14155. https://doi.org/10.1523/JNEUROSCI.2932-12.2012.
54. Liu, L., Zhang, K., Sandoval, H., Yamamoto, S., Jaiswal, M., Sanz, E., Li, Z., Hui, J., Graham, B.H., Quintana, A., and Bellen, H.J. (2015). Glial lipid droplets and ROS induced by mitochondrial defects promote neurodegeneration. Cell *160*, 177–190. https://doi.org/10.1016/j.cell.2014.12.019.
55. Duffy, J.B. (2002). GAL4 system in Drosophila: a fly geneticist's Swiss army knife. Genesis *34*, 1–15. https://doi.org/10.1002/gene.10150.
56. Brand, A.H., Manoukian, A.S., and Perrimon, N. (1994). Ectopic expression in Drosophila. Methods Cell Biol. *44*, 635–654. https://doi.org/10.1016/s0091-679x(08)60936-x.
57. Wilder, E.L. (2000). Ectopic expression in Drosophila. Methods Mol. Biol. *137*, 9–14. https://doi.org/10.1385/1-59259-066-7:9.
58. Baldridge, D., Wangler, M.F., Bowman, A.N., Yamamoto, S., Schedl, T., Pak, S.C., Postlethwait, J.H., Shin, J., Solnica-Krezel, L., Bellen, H.J., Westerfield, M.; and Undiagnosed Diseases Network (2021). Model organisms contribute to diagnosis and discovery in the undiagnosed diseases network: current state and a future vision. Orphanet J. Rare Dis. *16*, 206. https://doi.org/10.1186/s13023-021-01839-9.
59. Rentzsch, P., Witten, D., Cooper, G.M., Shendure, J., and Kircher, M. (2019). CADD: predicting the deleteriousness of variants throughout the human genome. Nucleic Acids Res. *47* (D1), D886–D894. https://doi.org/10.1093/nar/gky1016.
60. Kanca, O., Andrews, J.C., Lee, P.T., Patel, C., Braddock, S.R., Slavotinek, A.M., Cohen, J.S., Gubbels, C.S., Aldinger, K.A., Williams, J., et al.; Undiagnosed Diseases Network (2019). De Novo Variants in WDR37 Are Associated with Epilepsy, Colobomas, Dysmorphism, Developmental Delay, Intellectual Disability, and Cerebellar Hypoplasia. Am. J. Hum. Genet. *105*, 413–424. https://doi.org/10.1016/j.ajhg.2019.06.014.
61. Marcogliese, P.C., Shashi, V., Spillmann, R.C., Stong, N., Rosenfeld, J.A., Koenig, M.K., Martínez-Agosto, J.A., Herzog, M., Chen, A.H., Dickson, P.I., et al.; Program for Undiagnosed Diseases (UD-PrOZA); and Undiagnosed Diseases Network (2018). IRF2BPL Is Associated with Neurological Phenotypes. Am. J. Hum. Genet. *103*, 245–260. https://doi.org/10.1016/j.ajhg.2018.07.006.
62. Liu, N., Schoch, K., Luo, X., Pena, L.D.M., Bhavana, V.H., Kukolich, M.K., Stringer, S., Powis, Z., Radtke, K., Mroske, C., et al.; Undiagnosed Diseases Network (UDN) (2018). Functional variants in TBX2 are associated with a syndromic cardiovascular and skeletal developmental disorder. Hum. Mol. Genet. *27*, 2454–2465. https://doi.org/10.1093/hmg/ddy146.
63. Ravenscroft, T.A., Phillips, J.B., Fieg, E., Bajikar, S.S., Peirce, J., Wegner, J., Luna, A.A., Fox, E.J., Yan, Y.L., Rosenfeld, J.A., et al.; Undiagnosed Diseases Network (2021). Heterozygous loss-of-function variants significantly expand the phenotypes associated with loss of GDF11. Genet. Med. *23*, 1889–1900. https://doi.org/10.1038/s41436-021-01216-8.
64. Uehara, T., Sanuki, R., Ogura, Y., Yokoyama, A., Yoshida, T., Futagawa, H., Yoshihashi, H., Yamada, M., Suzuki, H., Takenouchi, T., et al. (2021). Recurrent NFIA K125E substitution represents a loss-of-function allele: Sensitive in vitro and in vivo assays for nontruncating alleles. Am. J. Med. Genet. A. *185*, 2084–2093. https://doi.org/10.1002/ajmg.a.62226.
65. Wang, J., Rousseau, J., Kim, E., Ehresmann, S., Cheng, Y.T., Duraine, L., Zuo, Z., Park, Y.J., Li-Kroeger, D., Bi, W., et al. (2019). Loss of Oxidation Resistance 1, OXR1, Is Associated with an Autosomal-Recessive Neurological Disease with Cerebellar Atrophy and Lysosomal Dysfunction. Am. J. Hum. Genet. *105*, 1237–1253. https://doi.org/10.1016/j.ajhg.2019.11.002.
66. Rooney, C., White, G., Nazgiewicz, A., Woodcock, S.A., Anderson, K.I., Ballestrem, C., and Malliri, A. (2010). The Rac activator STEF (Tiam2) regulates cell migration by microtubule-mediated focal adhesion disassembly. EMBO Rep. *11*, 292–298. https://doi.org/10.1038/embor.2010.10.
67. Otani, T., Ichii, T., Aono, S., and Takeichi, M. (2006). Cdc42 GEF Tuba regulates the junctional configuration of simple epithelial cells. J. Cell Biol. *175*, 135–146. https://doi.org/10.1083/jcb.200605012.
68. Viplav, A., Saha, T., Huertas, J., Selenschik, P., Ebrahimkutty, M.P., Grill, D., Lehrich, J., Hentschel, A., Biasizzo, M., Mengoni, S., et al. (2019). ArhGEF37 assists dynamin 2 during clathrin-mediated endocytosis. J. Cell Sci. *132*, jcs226530. https://doi.org/10.1242/jcs.226530.
69. Hoshino, M., Sone, M., Fukata, M., Kuroda, S., Kaibuchi, K., Nabeshima, Y., and Hama, C. (1999). Identification of the stef gene that encodes a novel guanine nucleotide exchange factor specific for Rac1. J. Biol. Chem. *274*, 17837–17844. https://doi.org/10.1074/jbc.274.25.17837.
70. Chiu, C.Y., Leng, S., Martin, K.A., Kim, E., Gorman, S., and Duhl, D.M. (1999). Cloning and characterization of T-cell lymphoma invasion and metastasis 2 (TIAM2), a novel guanine nucleotide exchange factor related to TIAM1. Genomics *61*, 66–73. https://doi.org/10.1006/geno.1999.5936.

71. Cook, D.R., Rossman, K.L., and Der, C.J. (2014). Rho guanine nucleotide exchange factors: regulators of Rho GTPase activity in development and disease. Oncogene *33*, 4021–4035. https://doi.org/10.1038/onc.2013.362.
72. Yoshizawa, M., Hoshino, M., Sone, M., and Nabeshima, Y. (2002). Expression of stef, an activator of Rac1, correlates with the stages of neuronal morphological development in the mouse brain. Mech. Dev. *113*, 65–68. https://doi.org/10.1016/s0925-4773(01)00650-5.
73. Goto, A., Hoshino, M., Matsuda, M., and Nakamura, T. (2011). Phosphorylation of STEF/Tiam2 by protein kinase A is critical for Rac1 activation and neurite outgrowth in dibutyryl cAMP-treated PC12D cells. Mol. Biol. Cell *22*, 1780–1790. https://doi.org/10.1091/mbc.E10-09-0783.
74. Suchowerska, A.K., and Fath, T. (2014). Cytoskeletal changes in diseases of the nervous system. Front. Biol. *9*, 5–17. https://doi.org/10.1007/s11515-014-1290-6.
75. Spence, E.F., and Soderling, S.H. (2015). Actin Out: Regulation of the Synaptic Cytoskeleton. J. Biol. Chem. *290*, 28613–28622. https://doi.org/10.1074/jbc.R115.655118.
76. Gambino, G., Rizzo, V., Giglia, G., Ferraro, G., and Sardo, P. (2020). Microtubule Dynamics and Neuronal Excitability: Advances on Cytoskeletal Components Implicated in Epileptic Phenomena. Cell. Mol. Neurobiol. https://doi.org/10.1007/s10571-020-00963-7.
77. Gardiner, J., and Marc, J. (2010). Disruption of normal cytoskeletal dynamics may play a key role in the pathogenesis of epilepsy. Neuroscientist *16*, 28–39. https://doi.org/10.1177/1073858409334422.
78. Gavrilovici, C., Jiang, Y., Kiroski, I., Teskey, G.C., Rho, J.M., and Nguyen, M.D. (2020). Postnatal Role of the Cytoskeleton in Adult Epileptogenesis. Cereb. Cortex Commun. *1*, tgaa024. https://doi.org/10.1093/texcom/tgaa024.
79. Lin, G., Lee, P.T., Chen, K., Mao, D., Tan, K.L., Zuo, Z., Lin, W.W., Wang, L., and Bellen, H.J. (2018). Phospholipase PLA2G6, a Parkinsonism-Associated Gene, Affects Vps26 and Vps35, Retromer Function, and Ceramide Levels, Similar to α-Synuclein Gain. Cell Metab. *28*, 605–618.e6. https://doi.org/10.1016/j.cmet.2018.05.019.
80. Yao, C.K., Liu, Y.T., Lee, I.C., Wang, Y.T., and Wu, P.Y. (2017). A Ca2+ channel differentially regulates Clathrin-mediated and activity-dependent bulk endocytosis. PLoS Biol. *15*, e2000931. https://doi.org/10.1371/journal.pbio.2000931.